AD NUMBER

AD464450

NEW LIMITATION CHANGE

TO

Approved for public release, distribution unlimited

FROM

Distribution authorized to U.S. Gov't. agencies and their contractors; Administrative/Operational Use; 13 APR 1965. Other requests shall be referred to Bureau of Naval Weapons, Washington, DC 20350.

AUTHORITY

18 Apr 1967, ST-A per USNOL ltr

NOLTR 65-33

THE EFFECTS OF CONFIGURATION AND CONFINEMENT ON BOOSTER CHARACTERISTICS

13 APRIL 1965

NOL

UNITED STATES NAVAL ORDNANCE LABORATORY, WHITE OAK, MARYLAND

NOLTR 65-33

NOTICE

Requests for additional copies by Agencies of the Department of Defense, their contractors, and other Government agencies should be directed to:

Defense Documentation Center (DDC)
Cameron Station
Alexandria, Virginia

Department of Defense contractors who have established DDC services or have their 'need-to-know' certified by the cognizant military agency of their project or contract should also request copies from DDC.

NOLTR 65-33

The Effects of Configuration and Confinement on Booster Characteristics

By

I. Jaffe and A. R. Clairmont

ABSTRACT: The purpose of this work was to examine the effect of certain changes in size, shape, and confinement on the effectiveness of tetryl boosters. Effectiveness was judged in two ways: by the booster's approximation to a plane-wave generator and by its initiating strength. Consequently the measurements made were of non-planarity (radius of curvature) of the detonation front emerging from the booster and of the shock velocity vs distance curves of the hydrodynamic disturbance it caused in Plexiglas.

The changes made in confinement and shape of two-inch-diam boosters caused no significant change in either performance property. Changes in booster length, however, had a marked effect. Booster effectiveness increases with increasing length and is still increasing at ℓ/d of 4 contrary to literature statements that curvature of the detonation front is constant at $\ell/d \geq 3$ and that booster strength becomes constant at $\ell/d \geq 1.5$. The validity of using truncated cones in place of cylindrical boosters in large-scale field tests of detonability was confirmed. The variation of 50% gap thickness with booster length (and corresponding invariance of critical initiating pressure), for a given test material, was quantitatively measured.

PUBLISHED JUNE 1965

APPROVED BY: Carl Boyars, Chief
Physical Chemistry Division
CHEMISTRY RESEARCH DEPARTMENT
U. S. NAVAL ORDNANCE LABORATORY
White Oak, Silver Spring, Maryland

The work of this report is one phase of a continuing investigation of the sensitivity of propellants and explosives. Observations were made on the effect of certain changes in size, shape, and confinement on the effectiveness of tetryl boosters. Several conclusions are made regarding the use of truncated boosters in place of cylindrical boosters, the correlation between length and shock planarity, and the relationship between length and booster efficiency. The investigation was carried out under Task RMMP-22 149/212 1/F009/06-11, Propellant and Ingredient Sensitivity.

R. E. ODENING
Captain, USN
Commander

ALBERT LIGHTBODY
By direction

TABLE OF CONTENTS

ILLUSTRATIONS

TABLE OF CONTENTS
(Cont)

FIGURES

The Effects of Configuration and Confinement on Booster Characteristics

By

I. Jaffe and A. R. Clairmont

INTRODUCTION

For large scale, critical diameter tests, replacement of the cylindrical booster by a truncated cone has been recommended (1); an equivalent stimulus delivered to the test material from approximately 1/3 the amount of booster explosive was desired. For the laboratory scale, gap sensitivity test (2), strong recommendations have been made to replace the current booster of length to diameter ratio, L/D = 1, with a cylinder of L/D ≥ 3. There is general agreement that an L/D of 3 or more is desirable to assure a build-up to steady state from a minimal shock initiation, but this does not seem relevant to the use of an adequately detonated booster in measuring the shock sensitivity of an acceptor test material (L/D ≥ 3). In other words, if the booster exhibits steady state detonation, the same value of critical pressure necessary to initiate the acceptor should be measured, regardless of booster length.

It was the intent of the present investigation to examine the effects of changes in size, shape and confinement on the booster effectiveness. The shape of the detonation wave front emerging from the booster and the shock it set up in Plexiglas* were used for this purpose. In addition to meeting these objectives, the data acquired serve to correct the following inexact statements in the literature:

1. that the curvature of the detonation front becomes constant after an L/. of about 3 (3);

2. that the 50% gap value for a booster of L/D = 0.637 will differ from that with an L/D = 1.274 by a constant thickness (4); and

3. that increasing the booster length beyond L/D = 1.5 will have no further effect (4).

---

* Manufactured by Rohm and Haas

EXPERIMENTAL PROCEDURE

A. The Wave Shape

Tetryl pellets (ρ_o = 1.51 ± 0.01 g/cc), 50.8 mm in diameter and 25.4 mm long, were stacked and cemented together at their periphery to form cylinders of various lengths. These cylinders were used unconfined or confined in steel pipes (50.8 mm I.D., 76.2 mm O.D.), or they were machined down to the shape of a truncated cone. The two bases of the truncated cones were kept constant at 9.5 mm diameter and 50.8 mm respectively. The angle of inclination of the cones varied with the length of the cone.

Figure 1 is a composite drawing showing the general arrangement used to observe the wave planarity of the various charges. A No. 6 blasting cap* was used to initiate the booster. The cap was lined up with the axis of the charge, and held in place by a cylindrical piece of wood (50.8 mm dia., 25 mm long), cemented to the base of the charge.

An aluminized Plexiglas flasher, 50.8 mm in diameter and 3.2 mm thick, was cemented at its periphery to the end of the charge. The thin layer of air sandwiched between the charge and the disc flashes when it is hit by the shock wave. The intensity of the flash increases the illumination, facilitating the recording of the wave shape by the smear camera. The camera views the shock front through a small transparent area, 3.2 mm wide, which divides the disc into four equal parts (see Fig. 1B).

To align the axis of the charge with the optical axis of the camera, a beam of light was projected back through the camera onto the aluminized surface of the flasher. The assembly was adjusted until the beam of light was reflected back on its incident path, placing the charge axis in line with the optical axis.

The procedure was changed to observe the shape of the shock wave at the end of a blasting cap or detonator. The cap was aligned in the manner described above, but since the illumination produced by the cap was too weak to obtain a positive smear record, the wave shape was followed by observing the interruption of reflected light off an aluminized disc 25.4 mm diam x 0.025 mm thick at the end of the detonator. The light source, an exploding

---

* Manufactured by Clin-Mathieson

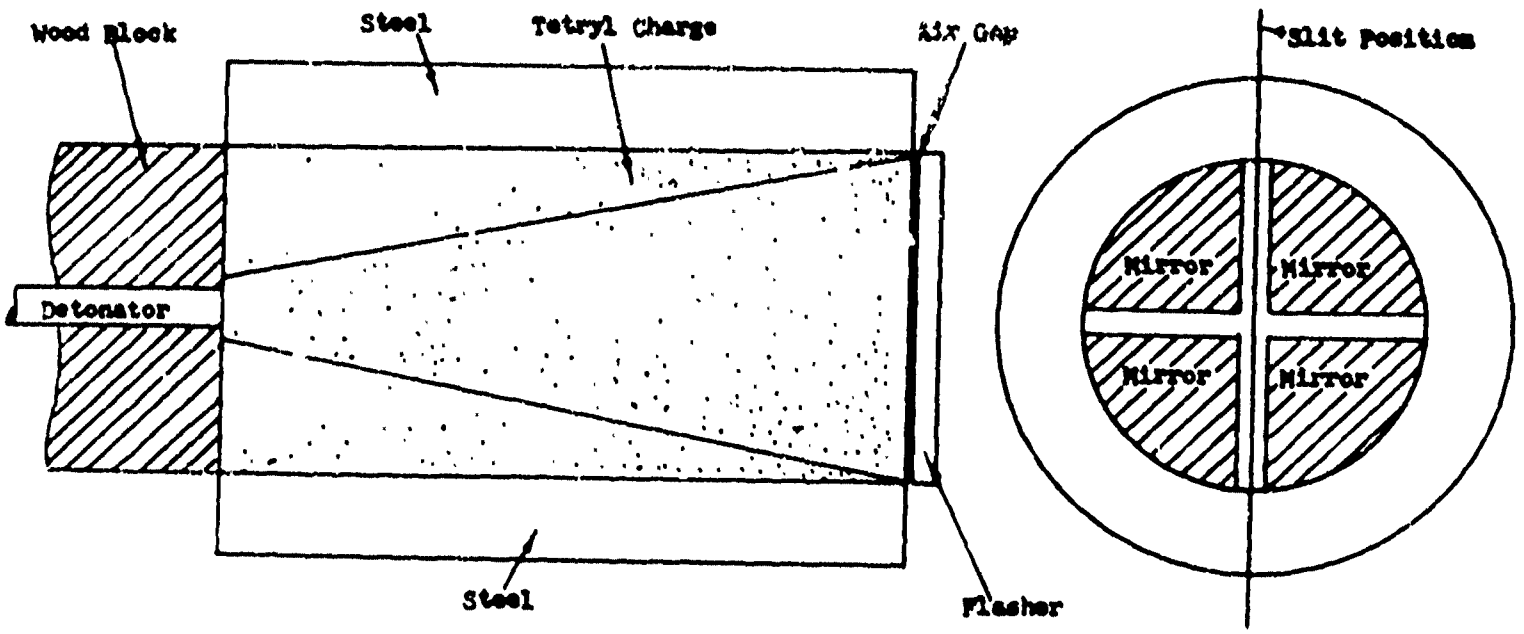

A. Composite Cross-section View

B. End View

NOLTR - 65-33

FIG. -1- EXPERIMENTAL ARRANGEMENT FOR WAVE PLANARITY MEASUREMENTS REPRESENTING CROSS-SECTIONAL VIEWS FOR CYLINDRICAL, CONICAL, AND CONFINED CYLINDRICAL CHARGES

wire, was arranged at an appropriate angle in front of the disc which reflected the beam along the optical axis into the camera. The writing speed of the smear camera was 1.32 mm/μsec.

B. The Shock Velocity

Figure 2 is a schematic diagram of the arrangement used to measure the shock velocity in a Plexiglas rod. The Plexiglas attenuators were machined from 50.6 mm flat stock to a cylinder approximately 52 mm in diameter, containing two parallel, opposing flats approximately 9-10 mm wide. The flats provide an undistorted optical path through the Plexiglas. Thin lines perpendicular to the axis of the cylinders, were inscribed on the flats to mark off known axial distances. A shield, consisting of Plexiglas 20 cm square and 2.5 cm thick, was used to prevent the reaction products from obstructing the view of the camera. The center portion of the shield was machined to a thickness of 3.2 mm (see Figure 2). This additional thickness of Plexiglas, carefully measured before each test, was considered as part of the total attenuation path.

A mirror, similar to the flasher used above, was fixed temporarily to a cylinder flat. The mirror was placed concentric with the midpoint taken along the length of the cylinder. The entire assembly was aligned, with the aid of the mirror, so that its longitudinal axis was perpendicular to the optical axis at the midpoint along the length of the cylinder.

The Plexiglas was back lighted by an exploding tungsten wire, across which 5000 volts were discharged. The wire, 0.05 mm diameter and 7[illegible] mm long, was strung in a 2.5 mm capillary tube and placed at the focal point of a 15 cm lens. The lens was used to collimate the light behind the cylinder. The cylinder was positioned approximately 10 cm in front of the lens.

RESULTS

Figures [illegible], [illegible], [illegible] are reproductions of the smear camera records magnified approximately [illegible] times. These particular records follow the development of the wave beginning at the end of the detonator, just prior to entering the tetryl charge, to the end of an unconfined, 20.[illegible] cm long, cylindrical charge. The grid lines, which are superimposed upon the original records, are equivalent to 1.[illegible] μsec/division along the time axis. The horizontal streak, in the center of the record, is a reference line which facilitates reading the records. In most instances, the distance can be measured to ± 0.1 mm and the time

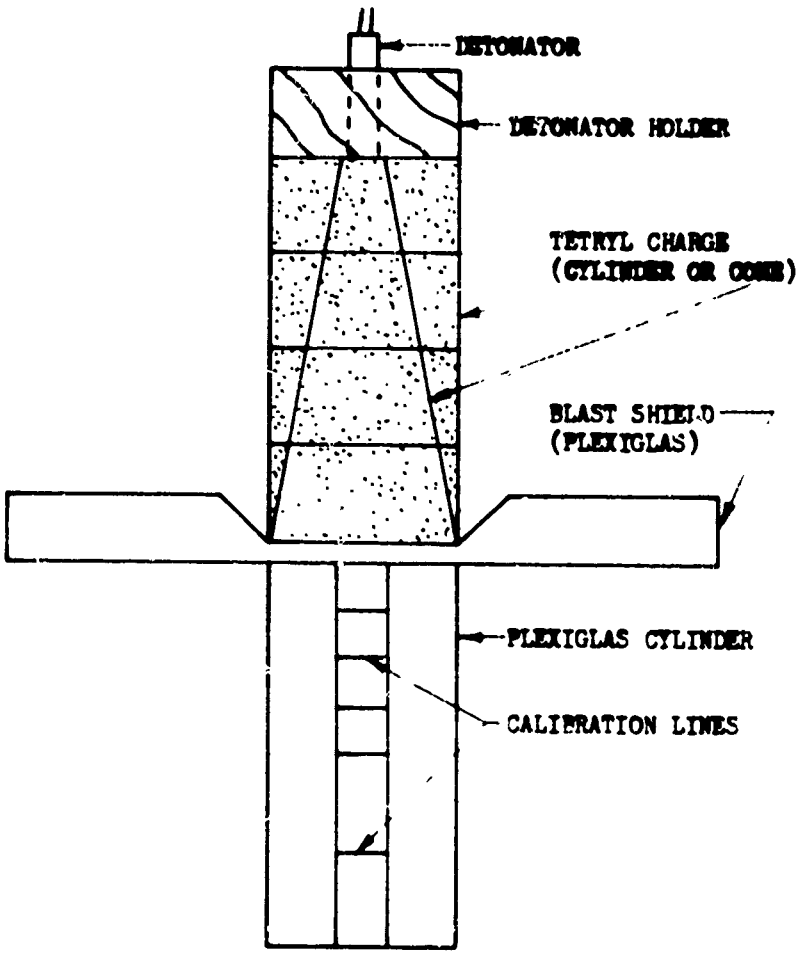

FIGURE -2- EXPERIMENTAL ARRANGEMENT FOR SHOCK ATTENUATION MEASUREMENTS

to 0.03 μsec. The results are listed in the Tables 1 - 7.

Figure 6 is a typical record obtained for the attenuation of a shock wave in a plexiglas rod. The distance, in this case, can be measured to ± 0.2 mm and the time to ± 0.03 μsec. The data have been recorded in the Tables 8 - 11.

DISCUSSION

The Wave Profile

Figures 3 - 5 show the progress and development of the wave front from its inception at the end of the detonator cap, to the end of a cylinder 50.8 mm in diameter and 20.32 cm long. The incident wave front off the cap is quite irregular and spread over an interval equal to 0.5 μsec (Fig. 3). The effect of this is to initiate the tetryl charge over a region approximately described by a circle whose diameter is somewhat greater than the diameter of the detonator (6 mm). The influence of the cap on the wave shape is quite apparent at the end of the 1.6 mm of tetryl and is still evident at the end of 3.2 mm of tetryl (Fig. 4). The irregularity in the front is completely lost, however, at the end of 12.7 mm of tetryl.

As the wave continues down the cylinder it flattens out. The edges of the front draw forward, and in line with the center. At the end of 20.3 cm of tetryl, there is a 0.2 μsec interval between the arrival of the center and the edges of the shock wave. The curves for the most part appear smooth and symmetrical about the center axis, and show no discontinuity at the boundaries of the cylinder due to lateral rarefactions.

The development of a detonation wave in the solid, tetryl cylinder, appears to be analogous to the expansion of a compression wave in a homogeneous medium such as water.* The charge is initiated at numerous points over a circular area of approximately 6 mm. Each point of initiation acts as a point source activating the material around it, creating minute areas (centers) of reactive particles. The result is determined at any given time by the envelope formed by the spheres expanding from the reacting centers. Given enough time and material, i.e., long enough path of travel, any irregularity in the detonation front disappears, and the wave front appears in the cylinder as a segment of a sphere which is expanding radially at constant velocity.

---

* Huygen's principle of wave construction

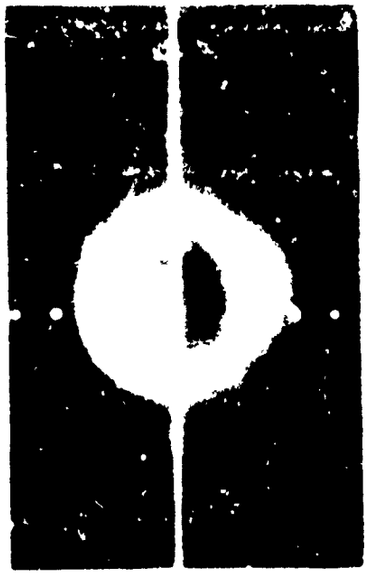

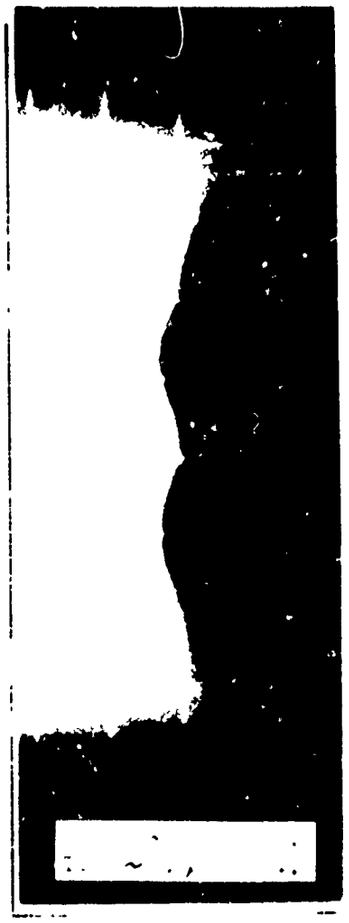

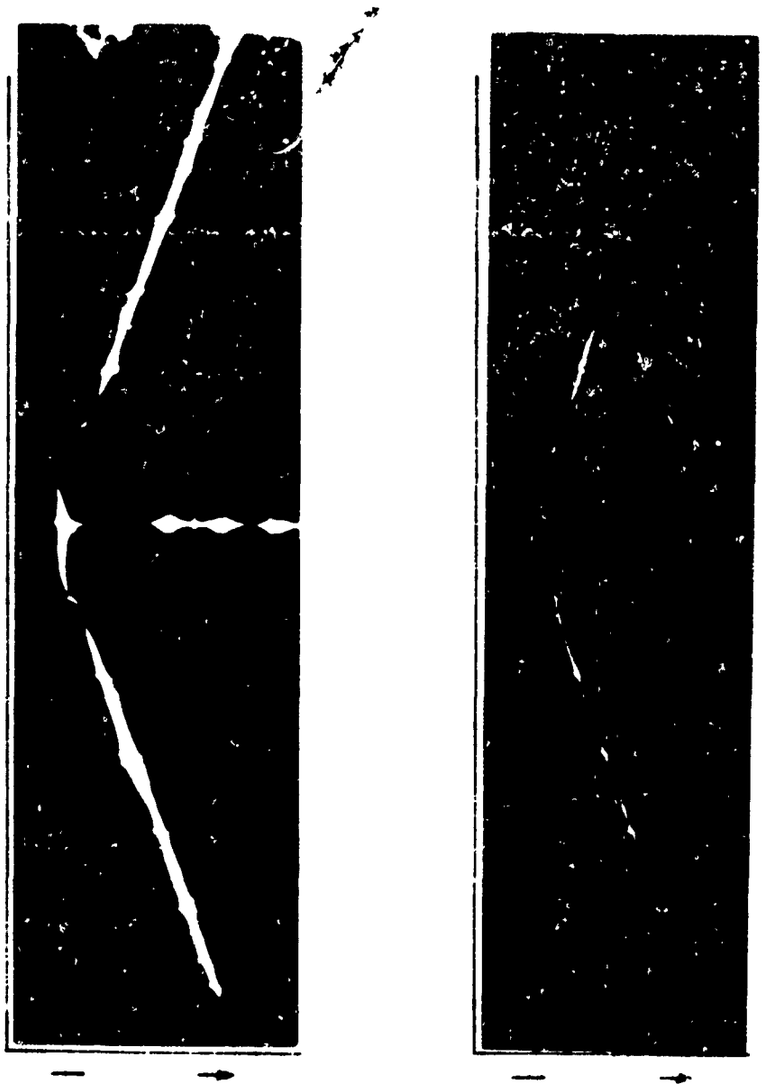

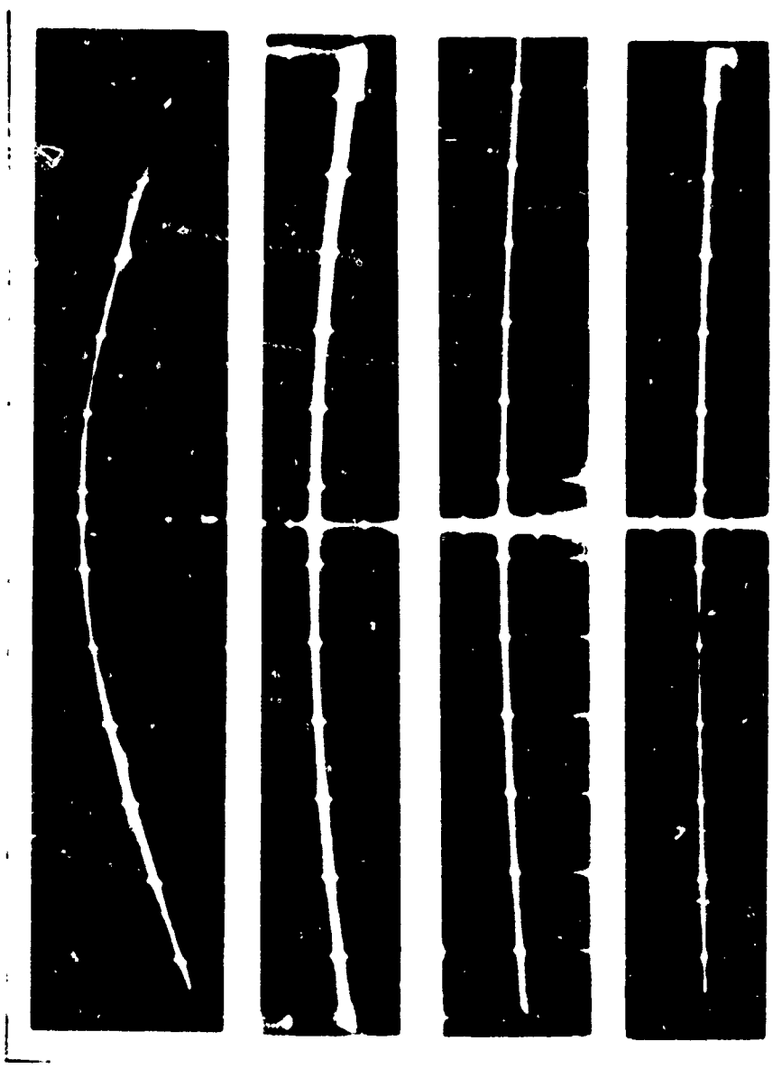

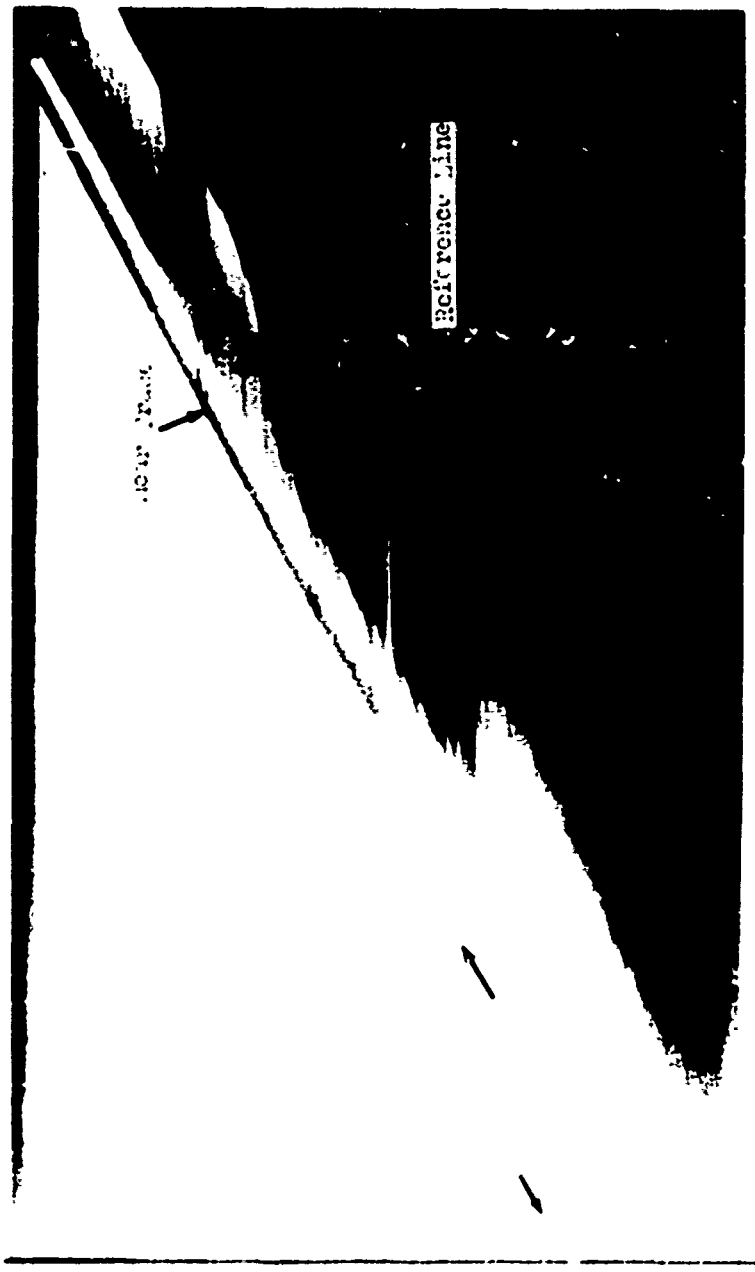

Time ——

ROUT ATTENUATED in a PLEXIGLAS CYLINDER

Assuming the shock wave is point initiated, spherical, and moving radially at a constant detonation velocity, it can be shown (5) that the following relationship holds:

$$R_i^2 = R_o^2 + Y_i^2 \tag{1}$$

or

$$\frac{R_i^2}{R_o^2} - \frac{Y_i^2}{R_o^2} = 1 \tag{2}$$

a rectangular hyperbola where

R_o = radius of curvature of the detonation front at time, t_o

t_o = the time that has elapsed from moment of initiation to the moment the shock front reaches the surface of the charge observed by the slit

R_i = radius of curvature of wave front at t_i

Y_i = distance front has traveled along the surface of the charge at time t_i

t_i = elapsed time as measured from the moment the shock front reaches the surface observed by the slit, i.e., time as measured on the smear camera trace

For a constant detonation velocity, equation (1) may be written as

$$(U_D t_o + U_D t_i)^2 = (U_D t_o)^2 + Y_i^2 \tag{3}$$

where

U_D = experimental detonation velocity

The value of detonation velocity used, U_D = 7.2 mm/μsec, had been previously measured (5). The data Y_i, t_i obtained from the experimental records and the detonation velocity (U_D) were supplied to the IBM 7090 computer. The computer chose the best equation, by a least squares method, to represent the data as a spherical front. Since no experimental record (Fig. 3 - 5)

showed any departure from the spherical shape at the lateral boundaries (edge effects), data over the entire front were used to obtain the best representative sphere. The results are presented in Table 12. In those instances where more than three experiments were made, a standard deviation of ± 3.2% (25.4 mm long bare cylinder) and ± 3.6% (50.8 mm long bare cylinder), were calculated. The mean value is given in all other cases. In most instances the spread of the data from the mean is about equal to or less than 3.5% with the exception of the 203.2 mm long unconfined cylinder (5%). This smaller precision is probably due to the proportionately smaller segment of the sphere used to calculate the radius of curvature in this long charge.

Figure 7 is a plot of the results listed in Table 12: radius of curvature on the axis as a function of the length of the unconfined cylinder. This curve is compared with a line representing the growth from a point initiation, of a spherical wave whose radius is equal to the length of the cylinder*. For any given length, the radius determined from the experimental results appears larger than the geometric radius (radius = length). The initiation of the charge occurred over an area approximately 6 mm in dia (Fig.4)and 1 mm from the beginning of the charge (5) rather than at a point at the base of the charge. This has the effect of increasing the apparent length of the charge. The experimentally derived radius is 1.09 times greater than charge length for the 25.4 mm and 50.8 mm charges, and 1.03 and 1.14 times larger for the 101.6 mm and 203.2 mm charges respectively. If the initiation for all the charges were the same, the largest deviation from the geometric radius would occur for the smallest length charge. However, the initiation front is dependent upon the detonator (Figs. 3 and 4). As a result the initial wave front in the tetryl is not planar, need not be symmetrical, nor need it be initiated over the same cross-sectional area for each charge (See Fig. 4). Thus the mode of initiation will affect the measurements. A combination of this experimental variation and the precision of the measurements can account for the apparent small departure of the detonation front curvature from spherical expansion (Fig. 7).

As the length of the charge increases, the radii of curvature continue to increase. A "steady state" radius which

---

* Continuous spherical expansion is to be expected if the reaction zone of the explosive has zero thickness; in this case, no rarefactions can catch up to (and affect) the reaction zone.

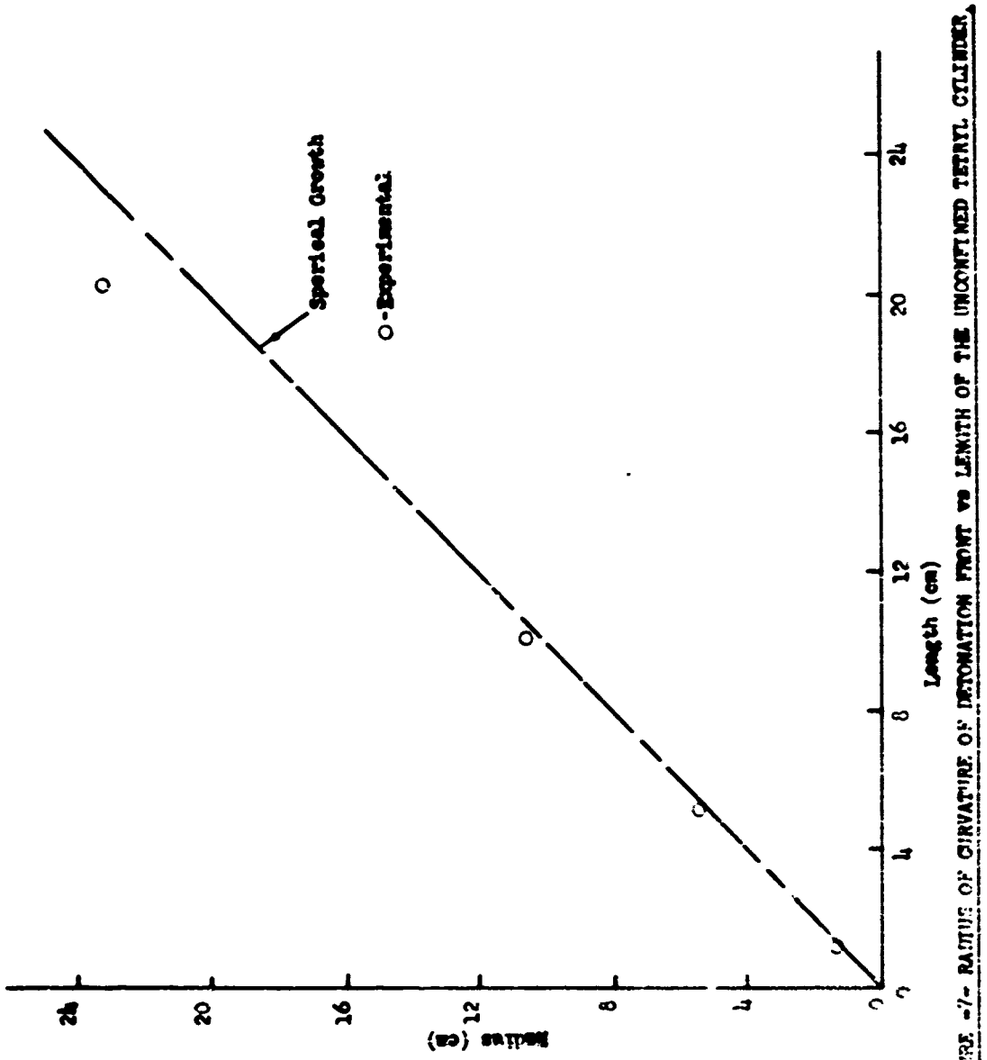

FIGURE -7- RADIUS OF CURVATURE OF DETONATION FRONT VS LENGTH OF THE UNCONFINED TETRYL CYLINDER

does not increase with an increase in charge length was not obtained for the range of charges studied. Because no significant departure from the curve for spherical expansion could be observed up to (L/D) = 4, the existence of such a steady state radius of curvature appears dubious. However, such a radius of curvature (constant, at an L/D greater than 2 to 3.5) has been reported for a number of "ideal" explosives (3).

The Effects of Booster Shape, Size, and Confinement on the Detonation Front

The physical states of the three boosters are quite different: a bare cylinder, a cylinder confined by a 1/2 inch thick steel wall, and a truncated cone whose mass is about 1/3 the mass of the cylinder. For a charge length of one radius (25.4 mm), the curvature of the detonation front should be the same for the cylindrical charges (confined and unconfined). It is only after the front has traveled 25.4 mm or more that the influence of the environment, giving rise to rarefactions for the unconfined charge and shock reflections for the confined charge, might become effective. In the conical charge, the detonation reaction is subjected to lateral rarefactions almost from the instant of initiation. The effects of these parameters on the shape of the detonation front are compared in Figure 8, which displays radius of curvature as a function of length for each of the different charges.

Considering the large differences in the boosters, the resultant changes in the shape of the detonation front (Fig. 8) are relatively small and are of the same size as the experimental error. The apparent differences at (L/D) > 2 are, however, generally in the direction to be expected for small effects of greater lateral rarefaction in the cone and lesser lateral rarefaction in the confined cylinder as compared, in both cases, to the unconfined cylinder.

Effect of Booster Changes on Explosive Loading

To observe the effects of a variation in booster configurations on the pressure or impulse loads produced by boosters, the attenuations of non-reactive shocks caused by the booster loading of Plexiglas rods (See Fig. 2) were measured and compared. The experimental data (Tables 8-11) were numerically curve fitted. The resulting distance-time equations were differentiated with respect to time to obtain the shock velocity in the Plexiglas. Current procedures for the data reduction are reported in greater detail in reference 6, App. II.

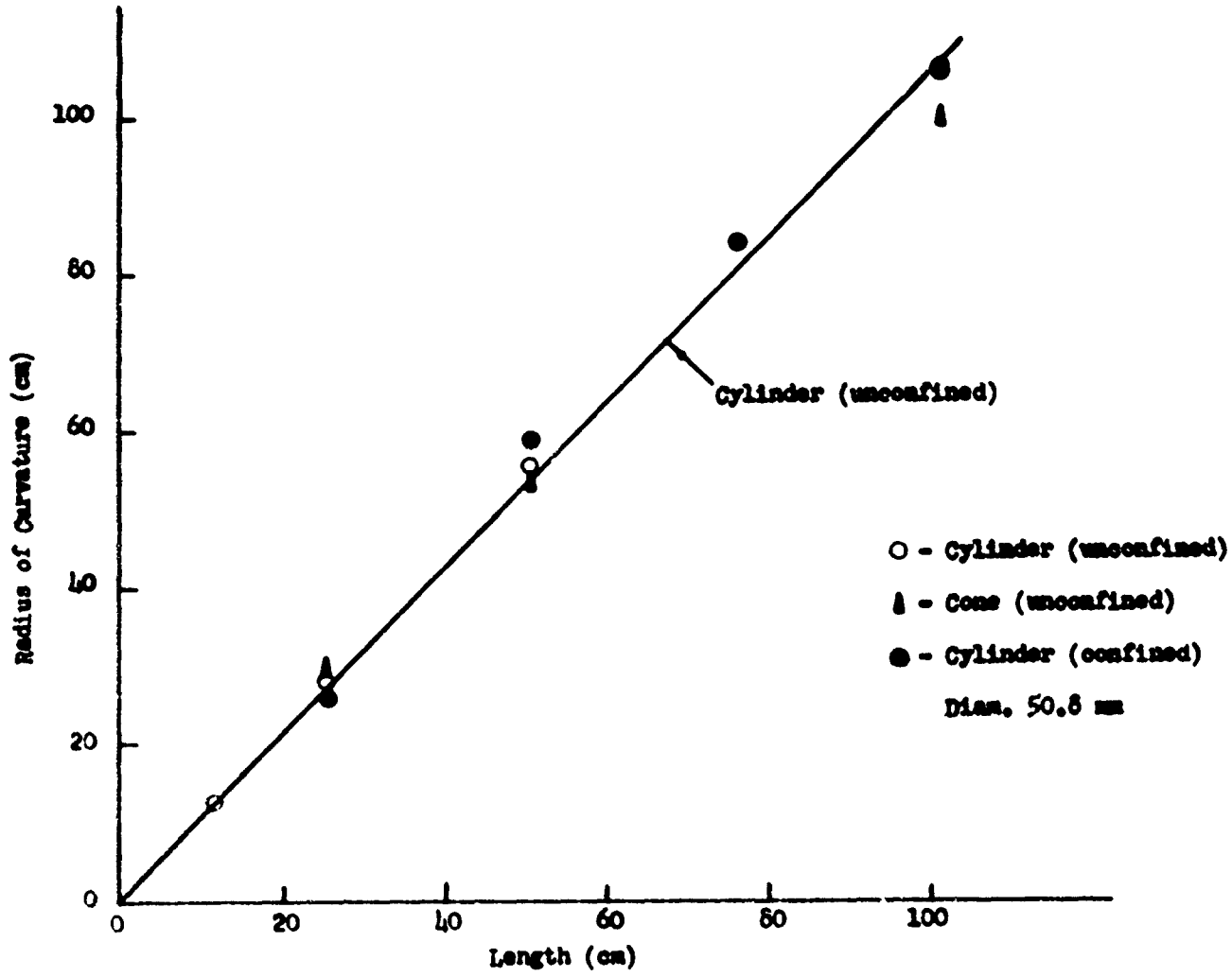

FIGURE 7 - COMPARISON OF THE RADII OF CURVATURE FOR THE THREE DIFFERENT TETRYL DONORS

Given the Hugoniot relationships for Plexiglas, which relate particle velocity, shock velocity and shock pressure, it is possible to compare the shock pressures obtained in the Plexiglas cylinder as a function of the booster used. However, the accuracy of the available experimental Hugoniots relating shock velocity and particle velocity are questionable. Moreover, because of the calculation required to derive the shock pressures from the shock velocities, the errors made in reading the experimental data and obtaining the shock velocities are then magnified by differing amounts throughout the pressure range studied. Consequently, shock velocities rather than pressures are compared here.

The experimental shock velocities as a function of time in Plexiglas shocked by charges of different lengths are given in Table 13 and are plotted in Figures 9 - 12. The value at zero time, i.e., at the tetryl-Plexiglas interface, is an extrapolated value. The first experimental measurement in the Plexiglas was made at about 5 mm from the interface. At this point the precision of the velocity is believed to be about + 5%; however, the error decreases with an increase in the length of the rod, and is approximately + 0.1 - 0.2% at 100 mm of Plexiglas. The time-dependent shock pressure amplitude in the Plexiglas will depend upon the impedance mismatch between the tetryl detonation products and Plexiglas and on the complete pressure-time history behind the detonation front. For a given booster in which the steady state has been achieved, the pressure-time profile behind the detonation front may be divided into two time intervals. The first is a short period of less than a microsecond in which the high shock pressure (von Neumann spike) at the detonation front falls to the detonation pressure at the end of the reaction zone (Chapman-Jouget point). In the second interval, which is much longer than the first, the pressure falls from the C.J. pressure to an ambient pressure. Theoretically, the first interval is reproducible, but the second may not be, as it depends upon size, shape, and/or confinement of the booster.

When the pressure-time profile behind the detonation wave is very steep, the velocity of the shock in the Plexiglas will attenuate extremely fast within a short distance past the interface. The initial and steepest portion of the attenuation curve will lie relatively close to the vertical axis of Figures 9 - 12; the most rapid attenuation occurs before the first experimental observation at 5 mm. Thus an extrapolation back to zero length of Plexiglas will not follow the true attenuation curve and will yield a shock velocity which is lower than the actual shock velocity at the interface. As the pressure-distance profile in the booster becomes less steep,

i.e., the booster is longer, the attenuation rate of the shock in the Plexiglas is reduced and the relative error in the extrapolated shock velocity at the interface is smaller. Of course it never approximates the pressure transmitted by the von Neumann spike, but it may approach that caused by the C-J pressure in the booster.

In each of Figures 9 and 10, the attenuation curves are compared for boosters having the same geometry but different lengths. In both cases, cylinder (Fig. 9) and cones (Fig. 10), the shock velocity at 5 mm of Plexiglas increased with an increase in charge length. The curves are shown as dashed lines in the interval 0 to 5 mm Plexiglas. The dashes indicate that this portion of the curve results from extrapolation into a region where experimental results could not be obtained. We know that this portion of the curve is fictitious because the boundary pressure transmitted from the tetryl booster must, in every case, be the same. Hence the attenuation in the first 5 mm of travel follows the qualitative pattern indicated by variation with booster length of the steepness of the Taylor wave following the detonation: greatest attenuation for the shortest booster.

Within the region of shock travel greater than 5 mm Plexiglas, the rates of attenuation are approximately the same for all three booster lengths. Of course, the apparent average attenuation over 5 to 70 mm path is greatest for the longest booster, but this results from considering the pressure drop from the extrapolated initial pressure which is much lower than the actual initial pressure.

For the region 5 to 100 mm Plexiglas, Figs. 9 and 10 show shock velocity (and pressure) decreasing with path length until the curves from different length boosters become experimentally coincident at about 50 mm and above. In Fig. 9, the three curves do not show as smooth a trend with variation in booster length as would be expected; in particular, there seems to be no levelling off of the initial (extrapolated) values with increasing booster length, as would be expected. The middle curve (paralleling the lower curve) seems to be slightly tipped so that it is too low at the boundary and too high at 50 mm and more. The calibration curve for the standard booster (50.8 mm long, (L/D) = 1) was derived from the greatest number of shots (five), and has been checked by Liddiard's work (7). Hence the apparent parallelism between this curve and that for the 101.6 mm booster probably arises from errors in the latter curve; the effect of the errors is to produce too small a slope in the initial part of the curve. Additional evidence of this appears in the comparison of analogous curves for cones and cylinders.

Figure 11 compares the calibration curves for the three boosters of 50.8 mm length. The three curves are, within experimental error, coincident for the first 50 mm of shock travel. Figure 12 makes the corresponding comparison for 101.6 mm cones and cylinders. Although there appears to be a

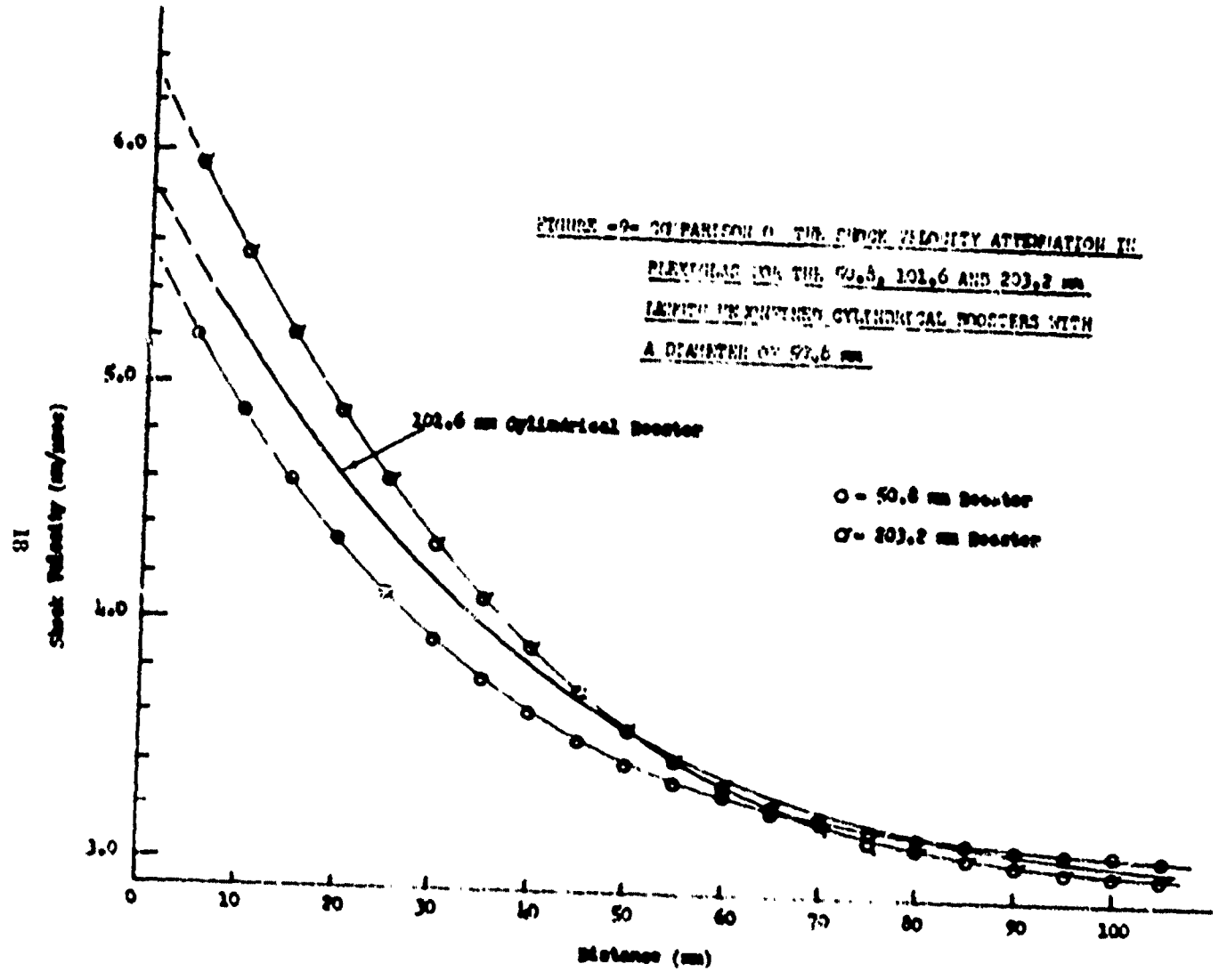

FIGURE -2- COMPARISON O... THE SHOCK VELOCITY ATTENUATION IN PLEXIGLAS FOR THE 50.8, 101.6 AND 203.2 mm LENGTH TO DIAMETER CYLINDRICAL BOOSTERS WITH A DIAMETER OF 97.6 mm

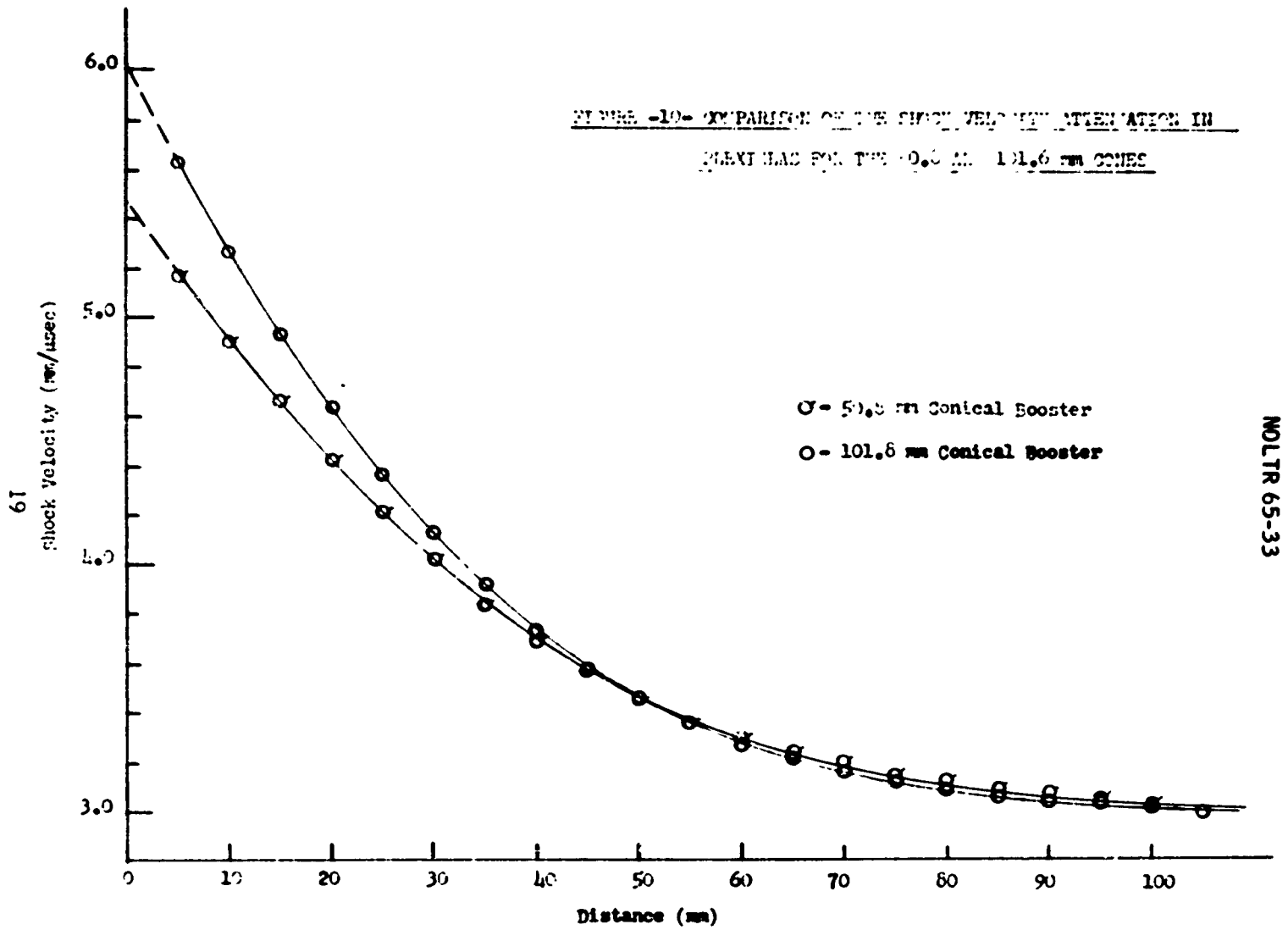

FIGURE -10- COMPARISON OF THE SHOCK VELOCITY ATTENUATION IN PLEXIGLAS FOR TWO 50.8 AND 101.6 mm CONES

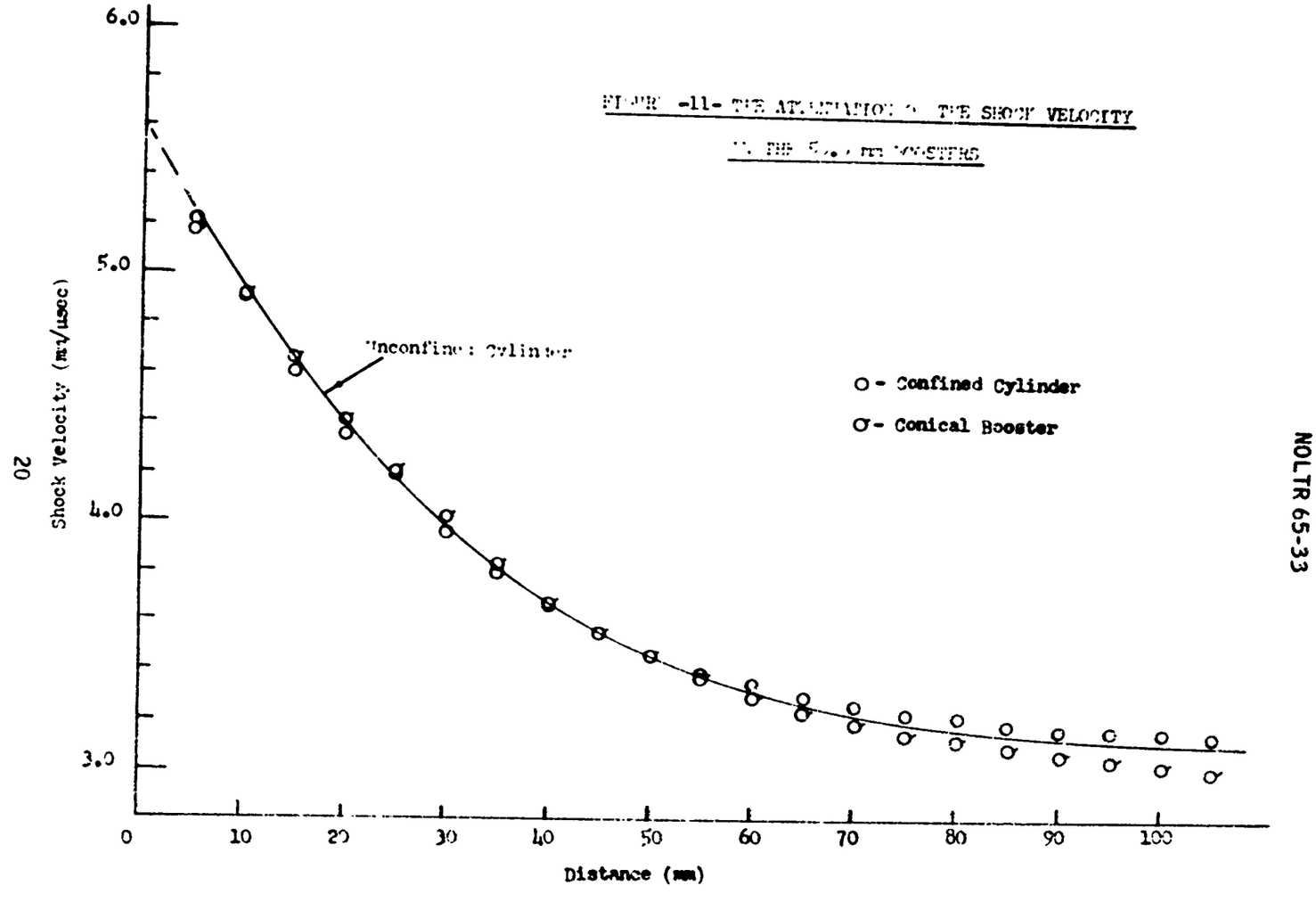

FIGURE -11- THE ATTENUATION OF THE SHOCK VELOCITY IN THE 5% PETN WAVETRS

NOLTR 65-33

FIGURE -12- THE ATTENUATION OF THE SHOCK VELOCITY IN THE 101.6 mm BOOSTERS

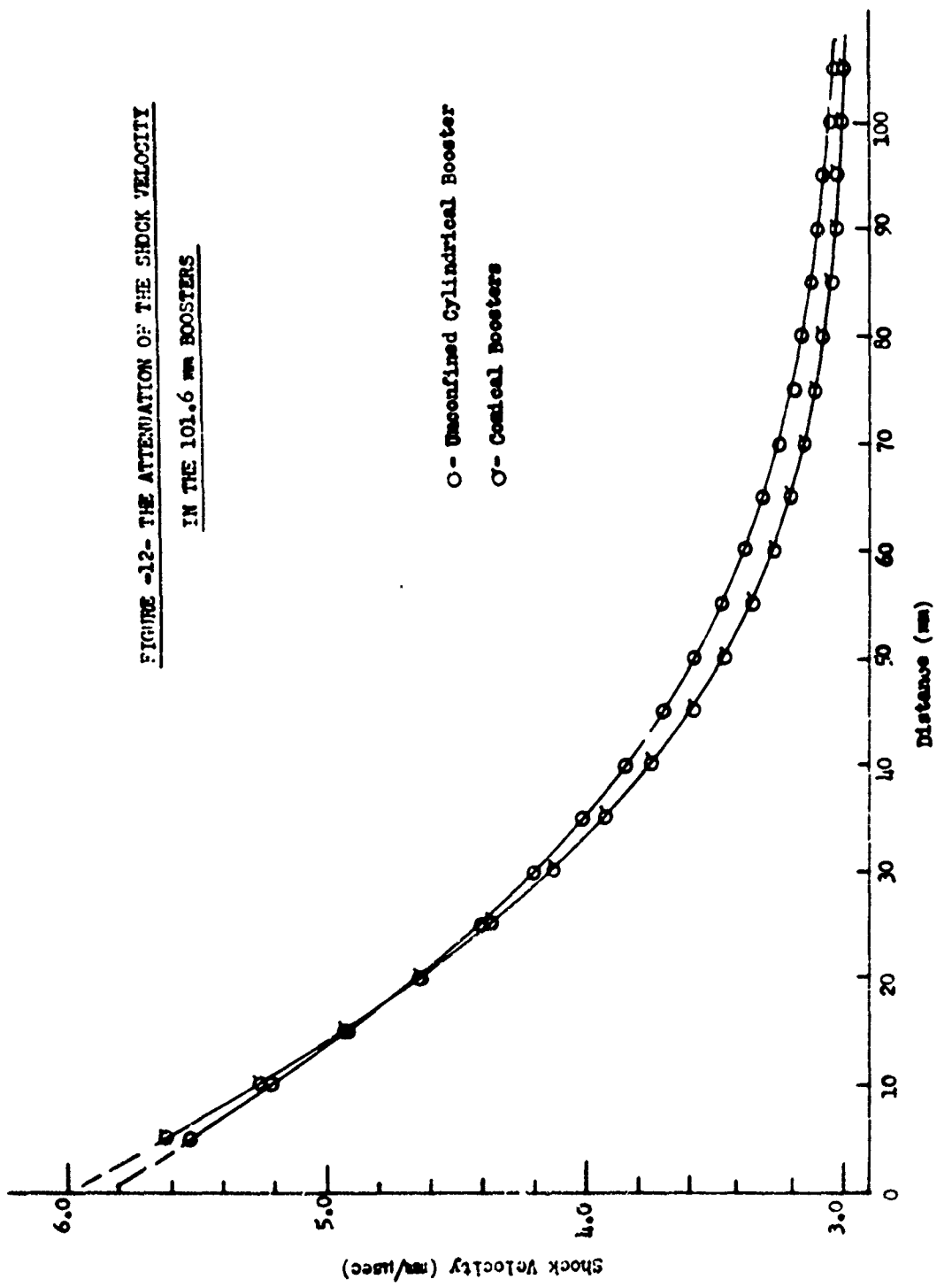

a greater difference than in Fig. 11, it is still within experimental error. Moreover, the apparent difference (stronger shock from cone than from cylinder) is, in this case, in the wrong direction. Since the curve for the 101.6 mm cylinder is already suspected to be in error by showing an insufficiently steep, initial slope, it is a reasonable working assumption that here, as well as in the case of the 50.8 mm boosters, the curves should be coincident for the first 50 mm, and that the curve for the cone happens to be closer to the true common curve than does that for the cylinder. Substitution of the 101.6 mm curve from the conical booster for that of the cylinder in Fig. 9 is a change within the experimental error which aligns the data to give smoother experimental trends. The validity of this substitution is supported by the gap test results shown in Table 14.

Three sets of explosive charges covering a range in shock sensitivity were prepared. Each was tested for gap sensitivity with the cylindrical tetryl boosters of 50.8 mm and of 101.6 mm length. For the 50.8 mm long boosters, the corresponding shock velocity at the end of the gap was taken from the standard calibration curve because, as argued above, this curve should be the more accurate. With this assumption, the 50% gap values obtained by use of the 101.6 mm long boosters then give three points on a calibration curve, shock velocity vs. gap thickness, for these longer boosters. Comparison can now be made of the curve indicated by the gap test values (columns 2 and 3 of Table 14) with those already obtained for the 101.6 mm long cone (column 4) and the 101.6 mm long cylinder (column 5). It is evident that the curve from the gap test values lies closer to that for the cone than to that for the cylinder.

Irrespective of the extent of the error in one of the curves, Figs. 9 to 12 supply much of the information sought in the study. Figs. 9 and 10 show that there will not generally be a simple relationship between the 50% gaps measured with different length donors. The trend is longer gap with longer booster, but the difference is greatest for insensitive materials (small gaps) and decreases to zero for the more sensitive acceptors. Substitution of one booster for another in a gap test requires a calibration for both boosters to explain the two sets of results, for they can be correlated only in terms of initiating pressures (or shock velocities), not by measured 50% gap thicknesses.

Figures 9 and 10 show the calibration curves for different booster lengths converging, and this is the expected trend. It is easy to see, however, that for small changes in L/D (0.637 to 1.274), tests over a limited range of gap might give 50% gap

values which differ by what appears to be a constant thickness, within experimental error.

Figure 9 shows that the boostering effectivensss increases with charge length, and that it is still increasing at (L/D) = 4. If the suggested correction is made to the middle curve, i.e., substitution of the curve obtained with the 101.6 mm cone, the rate of increase is beginning to fall off at (L/D) = 4.

Figures 11 and 12 show that the shock waves produced by the cylindrical and conical tetryl boosters of equal L/D are, within experimental error, the same for path lengths of up to 50 mm in Plexiglas. After longer paths through the attenuator, the curves show apparent differences according to the booster type. The maximum differences at high attenuation are in a region where conversion of shock velocity (U) to pressure by use of Hugoniot data is inadequate (6). Moreover, the greatest difference in U is 0.2 mm/μsec which is the order of magnitude of experimental error. More precise measurements of U accompanied by careful measurements of free surface velocity in the high attenuation region might establish whether the apparent difference is a true one; no further work has been done on it because this particular point is irrelevant to the purpose of the present investigation.

No experimentally significant differences were detected between the conical and cylindrical boosters of the same length either in the shape of their detonation front or in the shock pressures their detonation caused in thin layers of Plexiglas. Thus it would appear that in a practical test of explosives and propellants at zero gap a cylindrical booster may be replaced by a conical booster as long as the same L/D ratio is maintained. In the case of the truncated cone, the diameter of the larger base is used to compute L/D.

CONCLUSIONS

Several observations have been made. These are:

1. There is no significant difference between tetryl boosters, in the form of truncated cones or cylinders of the same length, in either curvature of the emerging detonation front or axial stimulus delivered to the acceptor at zero gap. Hence for large scale shock tests it is preferable to use a cone rather than a cylinder to reduce the weight of the required explosive charge.

2. Boosters of the same length but different geometry show similar shock attenuation in Plexiglas up to about 50 mm thickness of the attenuator.

3. There is no simple way to correlate gap test results obtained with boosters of different lengths without calibrating the booster-attenuator systems.

4. Although increasing booster length increases the measured 50% gap, the same initiating pressure for a given acceptor is measured in either case in the range $L/D \geq 1$.

5. The booster effectiveness definitely increases with length. It is still increasing at an $L/D = 4$.

6. The curvature of the detonation front in a finite, approximately point initiated charge shows no sign of attaining a constant value up to $L/D = 4$. Indeed, it is still following, within experimental precision, a spherical expansion.

ACKNOWLEDGEMENT

We wish to acknowledge the invaluable assistance and guidance given us by Dr. D. Price and Mr. J. W. Enig.

REFERENCES

(1) Explosives Hazard Classification Procedure, BuWeps Inst 8020.3, July 1962.

(2) D. Price and I. Jaffe, ARS Journal 31, 595-99 (1961).

(3) M. A. Cook, G. S. Horsley, R. T. Keyes, W. S. Partridge, and W. O. Ursenback, J. Appl. Phys. 27, 269-277 (1956).

(4) E. H. Eyster, L. C. Smith, and S. R. Walton, "The Sensitivity of High Explosives to Pure Shocks", NOLM 10,336, July 1949.

(5) A. R. Clairmont and I. Jaffe, "Analysis of the Optical Determination of Detonation Velocity in Short Charges", NOLTR 64-23, May 1964.

(6) I. Jaffe, J. Toscano and D. Price, "Behavior of Plexiglas Under Shock Loading by a Tetryl Donor", NOLTR 64-66, July 1964.

(7) T. S. Liddiard, Jr. and D. Price, NOLTR 65-43, in press.

TABLE 1 · Shock Front Profile · Unconfined Tetryl Cylinders
(12.06 mm and 25.4 mm lengths)

12.06 mm length		25.4 mm length							
Expt A-90		Expt A-14		Expt A-18		Expt A-20		Expt A-136	
Distance mm	Time μsec	Distance mm	Time μsec	Distance mm	Time μsec	Distance mm	Time μsec	Distance mm	Time μsec
25.4	2.25	25.0	1.32	23.4	1.17	23.6	1.21	25.0	1.28
22.9	1.93	22.3	1.09	18.2	.74	18.2	.75	22.5	1.06
20.3	1.62	17.3	0.66	13.1	.40	12.8	.39	20.0	.85
17.8	1.32	12.4	.34	7.8	.16	7.34	.14	17.5	.68
15.2	1.04	7.5	.11	2.7	.03	4.3	.06	15.0	.50
12.7	0.77	2.5	0	0	0	0	0	12.5	.34
10.2	.53	0	0	2.7	.04	3.8	.06	10.0	.22
7.6	.30	2.1	0	7.6	.14	8.8	.22	7.5	.11
0	0	7.2	.10	12.8	.36	14.2	.51	0	0
7.6	.23	12.1	.34	17.8	.70	19.8	.89	7.5	.11
10.2	.42	17.0	.66	22.9	1.11	25.0	1.35	10.0	.21
12.7	.64	21.9	1.07	25.2	1.34			12.5	.32
15.2	.88	25.2	1.42					15.0	.48
17.8	1.15							17.5	.66
20.3	1.44							20.0	.86
22.9	1.78							22.5	1.07
25.4	2.09							25.0	1.28

TABLE 2 - Shock Front Profile - Unconfined Tetryl Cylinders (50 mm long)

Expt A-16		Expt A-124		Expt A-130		Expt A-132	
Distance mm	Time µsec	Distance mm	Time µsec	Distance mm	Time µsec	Distance mm	Time µsec
25.0	0.70	25.0	0.76	25.0	0.73	25.0	0.76
23.6	.64	22.5	.64	22.5	.61	22.5	.64
21.6	.53	20.0	.51	20.0	.50	20.0	.51
19.4	.44	17.5	.38	17.5	.39	17.5	.38
16.6	.33	15.0	.30	15.0	.29	15.0	.30
13.8	.23	12.5	.22	12.5	.21	12.5	.22
11.1	.16	10.0	.16	10.0	.13	10.0	.16
9.3	.09	7.5	.09	7.5	.08	7.5	.09
6.8	.05	0	0	0	0	0	0
4.4	.03	7.5	.08	7.5	.07	7.5	.08
1.5	.01	10.0	.15	10.0	.11	10.0	.15
0	0	12.5	.21	12.5	.17	12.5	.21
1.4	.01	15.0	.29	15.0	.25	15.0	.29
3.0	.01	17.5	.39	17.5	.36	17.5	.39
5.0	.05	20.0	.50	20.0	.47	20.0	.50
7.9	.09	22.5	.61	22.5	.59	22.5	.61
10.3	.14	25.0	.76	25.0	.71	25.0	.76
12.8	.21						
15.3	.30						
17.6	.40						
19.8	.48						
22.5	.63						
25.7	.77						

TABLE 3 - Shock Front Profile - Unconfined Tetryl Cylinders (101.6 mm long)

Expt A-22		Expt A-23		Expt A-24	
Distance mm	Time μsec	Distance mm	Time μsec	Distance mm	Time μsec
25.0	0.36	25.2	0.41	24.6	0.35
21.0	.25	22.0	.34	22.0	.29
18.8	.20	20.0	.27	19.1	.22
16.0	.13	17.2	.19	17.0	.16
13.6	.08	15.1	.14	14.4	.13
11.1	.05	12.2	.10	12.1	.08
0	0	9.8	.05	8.3	.06
8.4	.05	7.3	.04	5.1	.03
10.8	.09	3.4	.01	0	0
13.2	.15	0	0	4.6	.02
15.7	.20	5.7	.01	7.4	.05
18.1	.27	8.5	.03	10.6	.08
20.7	.33	12.2	.07	13.5	.14
23.0	.39	14.8	.11	15.4	.18
25.4	.47	17.1	.16	17.4	.22
		19.7	.23	19.7	.29
		21.9	.29	22.4	.37
		25.1	.37	25.1	.45

TABLE 4 - Shock Front Profile - Unconfined Tetryl Cylinders (203.2 mm long)

Expt. No.	A-47	A-48	A-52
Distance mm	Time µsec	Time µsec	Time µsec
25.4	0.20	.19	.21
24.1	.18	.18	.20
22.9	.17	.15	.18
22.0	.15	.14	.16
20.3	.14	.13	.14
19.0	.12	.11	.14
17.8	.11	.11	.12
16.5	.09	.09	.11
15.2	.08	.08	.09
14.0	.07	.06	.08
12.7	.06	.05	.06
11.4	.04	.04	.05
10.2	.03	.03	.04
0	0	0	0
10.2	.03	.03	.04
11.4	.05	.05	.05
12.7	.06	.06	.07
14.0	.07	.08	.08
15.2	.08	.08	.09
16.5	.09	.09	.10
17.8	.11	.11	.12
19.0	.13	.12	.12
20.3	.14	.13	.14
22.0	.15	.15	.16
22.9	.17	.16	.17
24.1	.18	.18	.18
25.0	.20	.19	.20

TABLE 5 - Shock Front Profile - Confined Tetryl Cylinders*
(25.4 mm long and 50.8 mm long)

Length	25.4 mm			50.8 mm			
Expt No.	A-125	A-133	A-134	Expt No.	A 69	A-71	A-74
Distance mm	Time µsec	Time µsec	Time µsec	Distance mm	Time µsec	Time µsec	Time µsec
25.0	1.37	1.36	1.37	25.4	0.66	0.82	0.71
22.5	1.13	1.10	1.13	22.9	.54	.68	.55
20.0	0.91	.88	.91	20.3	.43	.56	.44
17.5	.69	.68	.70	17.8	.33	.45	.32
15.0	.51	.51	.51	15.2	.24	.32	.23
12.5	.32	.35	.35	12.7	.17	.23	.17
10.0	.22	.22	.22	10.2	.11	.16	.11
7.5	.12	.11	.12	0	-	-	-
0	-	-	-	10.2	.14	.12	.13
7.5	.11	.11	.12	12.7	.22	.19	.21
10.0	.20	.21	.23	15.2	.31	.26	.30
12.5	.31	.32	.32	17.8	.40	.37	.41
15.0	.41	.43	.50	20.3	.52	.46	.51
17.5	.60	.64	.70	22.9	.63	.59	.63
20.0	.87	.90	.90	25.4	.82	.70	.77
22.5	1.11	1.10	1.11				
25.0	1.36	1.37	1.34				

* Confinement consists of steel tube 12.7 mm thick

TABLE 6 - Shock Front Profile - Confined Tetryl Cylinders (76.2 mm and 101.6 mm long)

Length	76.2 mm			101.6 mm			
Expt No.	A-170	A-171	A-172	Expt No.	A-127	A-129	A-137
Distance mm	Time μsec	Time μsec	Time μsec	Distance mm	Time μsec	Time μsec	Time μsec
25.4	0.55	0.54	0.45	25.0	0.40	0.39	0.42
22.9	.44	.45	.36	22.5	.33	.32	.34
20.3	.34	.36	.26	20.0	.26	.26	.28
17.8	.26	.27	.20	17.5	.21	.20	.22
15.2	.18	.20	.14	15.0	.15	.15	.15
12.7	.13	.15	.09	12.5	.10	.09	.11
10.2	.08	.10	.04	10.0	.07	.07	.07
7.6	.04	.06	.02	7.5	.03	.02	.04
5.1	.02	.03	.01	0	-	-	-
0	-	-	-	7.5	.03	.04	.03
5.1	.01	.02	.04	10.0	.07	.08	.07
7.6	.04	.04	.08	12.5	.09	.11	.10
10.2	.07	.08	.12	15.0	.15	.15	.15
12.7	.11	.14	.17	17.5	.20	.20	.20
15.2	.17	.19	.24	20.0	.26	.26	.26
17.8	.23	.25	.32	22.5	.32	.39	.33
20.3	.31	.32	.40	25.0	.39	.39	.41
22.9	.40	.42	.48				
25.4	.49	.51	.58				

TABLE 7 - Shock Front Profile - Unconfined Cones*
(25.4 mm, 50.8 mm and 101.6 mm long)

Length	25.4 mm			50.8 mm			101.6 mm		
Expt No.	A-54	A-57	A-60	A-53	A-55	A-59	A-66	A-67	A-68
Distance mm	Time µsec	Time µsec	Time µsec	Time µsec	Time µsec	Time µsec	Time µsec	Time µsec	Time µsec
25.4	1.33	1.40	1.44	0.76	0.77	0.76	0.39	0.47	0.36
22.9	1.06	1.16	1.18	.61	.64	.64	.31	.38	.27
20.3	.84	.94	.96	.49	.50	.51	.24	.30	.20
17.8	.64	.74	.76	.38	.39	.39	.18	.23	.14
15.2	.49	.58	.57	.27	.29	.30	.14	.18	.10
12.7	.35	.44	.44	.18	.19	.19	.08	.13	.08
10.2	.23	.31	.30	.11	.12	.11	.06	.08	.04
7.6	.14	.21	.20	.08	.08	.07	-	-	-
0	-	-	-	-	-	-	-	-	-
7.6	.17	.16	.13	.08	.08	.08	-	-	-
10.2	.30	.25	.22	.14	.14	.14	.09	.06	.11
12.7	.42	.37	.32	.21	.23	.23	.12	.10	.14
15.2	.58	.52	.44	.30	.33	.32	.16	.15	.21
17.8	.75	.70	.59	.42	.43	.45	.22	.21	.27
20.3	.95	.83	.76	.53	.54	.56	.29	.29	.36
22.9	1.18	1.07	.98	.67	.68	.69	.38	.37	.45
25.4	1.40	1.30	1.16	.82	.80	.83	.47	.45	.54

* Apex 9.5 mm diameter - Base 50.8 mm diameter

TABLE 6 - Shock Attenuation in Plexiglas - Unconfined Tetryl Cylinders
(50.8 mm long)

Expt A-144		Expt A-145		Expt A-147		Expt A-175		Expt A 176	
Time μsec	Distance mm	Time μsec	Distance mm	Time μsec	Distance mm	Time μsec	Distance mm	Time μsec	Distance mm
0.57	3.18	0.52	3.1	0.52	3.18	0.62	3.12	0.62	3.12
1.75	9.53	1.71	8.1	1.71	7.10	1.52	8.20	1.52	8.20
3.09	15.88	2.10	11.1	2.09	11.18	2.74	13.28	2.70	13.28
4.49	22.58	2.90	15.1	2.96	15.18	3.83	18.36	3.75	18.36
5.98	28.58	3.74	19.1	3.94	19.18	4.94	23.44	4.94	23.44
7.50	34.98	4.75	23.1	4.74	23.18	6.18	28.52	6.14	28.52
9.47	41.28	6.00	28.1	6.00	28.18	7.47	33.60	7.41	33.60
12.19	53.98	7.24	33.1	7.24	33.18	8.73	38.68	8.77	38.68
14.74	66.68	8.55	38.1	8.54	38.18	10.15	43.76	10.17	43.76
17.72	79.38	10.02	43.1	10.01	43.18	11.62	48.84	11.62	48.84
20.80	92.08	11.47	48.1	11.46	48.18	13.06	53.92	13.09	53.92
23.49	104.78	12.98	53.18	12.98	53.18	14.61	59.00	14.63	59.00
		15.98	63.18	15.98	63.18	16.10	64.08	16.18	64.08
		18.98	73.18	18.97	73.18	17.66	69.16	17.74	69.16
		22.14	83.18	22.14	83.18	19.25	74.24	19.33	74.24
		25.36	93.18	25.35	93.18	20.78	79.32	20.93	79.32
		28.56	103.18	28.55	103.18				
		29.06	104.78	29.06	104.78	22.44	84.40	22.54	84.10
						24.03	89.48	24.13	89.48
						25.63	94.56	25.70	94.56
						27.23	99.64	27.32	99.64
						28.90	104.72	29.01	104.72
						30.53	109.80	30.64	109.80
						32.21	114.88	32.30	114.88
						33.84	119.96	33.96	119.96
						35.52	125.04	35.67	125.04
						37.18	130.12	37.30	130.12

TABLE 9 - Shock Attenuation in Plexiglas - Tetryl Cylinders - Unconfined (101.6 mm and 203.2 mm long)

50.8 mm dia x 101.6 mm long				50.8 mm dia x 203.4 mm long			
Expt A-169		Expt A-140		Expt A-177		Expt A-180	
Time μsec	Distance mm	Time μsec	Distance mm	Time μsec	Distance mm	Time μsec	Distance mm
0.86	5.0	0.60	3.4	0.55	3.2	0.55	3.2
1.79	10.0	1.83	9.7	1.12	6.4	1.11	6.4
2.77	15.0	3.06	16.0	1.67	9.5	1.67	9.5
3.82	20.0	4.36	22.4	2.28	12.7	2.26	12.7
4.96	25.0	5.74	28.8	2.90	15.9	2.87	15.9
6.10	30.0	7.28	35.1	3.51	19.0	3.48	19.0
7.34	35.0	8.91	41.4	4.13	22.2	4.10	22.2
8.66	40.0	10.76	47.8	4.74	25.4	4.73	25.4
10.09	45.0	12.71	54.2	5.44	28.6	5.40	28.6
11.50	50.0	16.60	66.8	6.07	31.8	6.07	31.8
13.01	55.0	20.61	79.6	6.80	34.9	6.80	34.9
14.53	60.0	24.71	92.2	7.58	38.1	7.54	38.1
16.04	65.0	28.85	105.0	8.34	41.3	8.34	41.3
17.55	70.0			9.20	44.4	9.15	44.4
19.12	75.0			10.04	47.6	10.09	47.6
20.74	80.0			10.93	50.8	11.00	50.8
22.39	85.0			11.96	54.0	12.01	54.0
24.02	90.0			12.89	57.15	12.98	57.15
25.63	95.0			13.90	60.3	13.95	60.3
27.27	100.0			14.83	63.5	14.88	63.5
28.75	104.5			15.79	66.7	15.90	66.7
				16.76	69.8	16.87	69.8
				17.72	73.0	17.88	73.0
				18.68	76.2	18.84	76.2
				19.70	79.4	19.88	79.4
				20.74	82.6	20.89	82.6
				21.74	85.7	21.90	85.7
				22.78	88.9	22.94	88.9
				23.78	92.1	23.95	92.1
				24.84	95.2	25.00	95.2
				25.89	98.4	26.00	98.4
				26.96	101.6	27.00	101.6
				27.97	104.7	27.[illegible]	104.8

TABLE 10 - Shock Attenuation in Plexiglas - Tetryl Cylinders - Confined (50.8 mm long)

50.8 mm dia x 50.8 mm long in 12.7 mm thick steel			
Expt A-173		Expt A-174	
Time μsec	Distance mm	Time μsec	Distance mm
0.92	5.0	0.91	5.0
1.94	10.0	1.95	10.0
2.97	15.0	2.97	15.0
4.11	20.0	4.12	20.0
5.30	25.0	5.30	25.0
6.56	30.0	6.55	30.0
7.78	35.0	7.79	35.0
9.12	40.0	9.16	40.0
10.55	45.0	10.52	45.0
11.95	50.0	12.02	50.0
13.45	55.0	13.51	55.0
14.92	60.0	14.92	60.0
16.46	65.0	16.48	65.0
17.95	70.0	17.96	70.0
19.53	75.0	19.52	75.0
21.02	80.0	21.07	80.0
22.57	85.0	22.60	85.0
24.13	90.0	24.14	90.0
25.71	95.0	25.72	95.0
27.32	100.0	27.24	100.0
28.93	105.0	28.83	105.0

TABLE 11 - Shock Attenuation in Plexiglas - Tetryl Cones - Unconfined

Cone - 50.8 mm long				Cone - 101.6 mm long			
Expt A-138		Expt A-139		Expt A-147		Expt A-153	
Time μsec	Distance mm	Time μsec	Distance mm	Time μsec	Distance mm	Time μsec	Distance mm
0.68	3.3	0.68	3.3	0.62	3.2	0.62	3.2
1.91	9.6	1.91	9.6	1.85	9.5	1.85	9.5
3.23	16.0	3.23	16.0	3.06	15.9	3.06	15.9
4.63	22.3	4.63	22.4	4.36	22.5	4.37	22.5
6.12	28.7	6.12	28.7	5.73	28.6	5.73	28.6
7.73	35.0	7.73	35.1	7.20	34.9	7.20	34.9
9.40	41.4	9.40	41.4	8.82	41.3	8.83	41.3
11.21	47.7	11.21	47.7	10.58	47.6	10.60	47.6
13.11	54.1	13.11	54.1	12.47	54.0	12.48	54.0
17.00	66.8	17.0	66.8	16.29	66.7	16.31	66.7
20.92	79.5	20.92	79.5	20.20	79.4	20.22	79.4
25.10	92.2	25.10	92.2	22.24	92.1	24.27	92.1
29.18	104.9	29.18	104.9	28.28	104.8	28.31	104.8

TABLE 12 - Computed Radii for the Shock Front Profiles

Length of Charge mm	Shot No. A-	Radii of Curvature of Unconfined Cylinder mm	Shot No.	Radii of Curvature of Cones mm	Shot No.	Radii of Curvature of Confined Cylinder mm
12.06	90	12.6				
25.4	14 18 20 136	26.6 28.6 28.0 28.2 Mean 27.8 ± 3.2%*	54 57 60	28.7 30.0 31.0 Mean 29.9	125 133 134	25.9 26.4 26.3 Mean 26.2
50.8	15 16 21 130 132 124	52.0 57.3 53.4 57.2 54.9 56.6 Mean 55.2 ± 3.6%*	53 55 59	54.0 54.0 52.6 Mean 53.5	69 71 74	61.9 57.1 57.8 Mean 58.9
76.2					170 171 172	83.2 83.9 85.0 Mean 84.0
101.6	22 23 24	102.6 107.2 106.6 Mean 105.4	66 67 68	102.0 97.4 100.6 Mean 100.0	127 129 137	106.0 110.4 103.1 Mean 106.5
203.2	47 48 52	223.0 241.0 230.1 Mean 231.4				

* Standard deviation

TABLE 13 - Shock Velocity in Plexiglas vs Distance

Size	50.8 mm			101.6 mm		203.2 mm
Shape	Unconfined Cylinder	Confined Cylinder	Cone	Unconfined Cylinder	Cone	Unconfined Cylinder
Time μsec	Velocity mm/μsec	Velocity mm/μsec	Velocity mm/μsec	Velocity mm/μsec	Velocity mm/μsec	Velocity mm/μsec
0	5.6	5.6	5.4	5.9	6.0	6.4
5	5.24	5.21	5.16	5.52	5.62	5.97
10	4.92	4.39	4.89	5.20	5.26	5.59
15	4.63	4.59	4.65	4.91	4.93	5.25
20	4.38	4.34	4.41	4.65	4.63	4.93
25	4.16	4.18	4.20	4.40	4.36	4.64
30	3.96	3.94	4.01	4.20	4.12	4.37
35	3.80	3.78	3.83	4.01	3.91	4.14
40	3.66	3.65	3.67	3.84	3.73	3.93
45	3.54	3.54	3.55	3.69	3.57	3.75
50	3.44	3.46	3.44	3.57	3.45	3.59
55	3.38	3.39	3.35	3.47	3.35	3.47
60	3.32	3.34	3.28	3.38	3.26	3.36
65	3.26	3.29	3.22	3.31	3.20	3.28
70	3.22	3.26	3.18	3.25	3.14	3.21
75	3.18	3.23	3.14	3.19	3.10	3.15
80	3.16	3.21	3.11	3.16	3.07	3.11
85	3.14	3.18	3.08	3.12	3 04	3.07
90	3.12	3.17	3.06	3.10	3.02	3.04
95	3.11	3.16	3.04	3.08	3.01	3.02
100	3.10	3.15	3.02	3.05	3.00	3.01
105	3.09	3.14	2.99	3.04	2.99	3.00

TABLE 14 - Comparison of 50% Gap Values Obtained with Different Tetryl Boosters

Acceptor	50% Gap No. Cards mm	Shock Velocity[c] at end of gap mm/μsec	50% Gap Values Predicted from Curves	
			101.6 mm cone[d] mm	101.6 mm cylinder mm
NQ(Lot 443) ρ_o = 1.612				
a	47(11.9)	4.81		
b	68(17.3)		17.0	17.0
NQ(Lot 510) ρ_o = 1.377				
a	113(28.7)	4.02		
b	131(33.2)		32.3	34.7
Cast TNT(Lot 457) ρ_o = 1.607				
a	135(34.3)	3.82		
b	145(36.8)		37.3	40.5

a Tetryl boosters Nb 1878-125*, ρ_o = 1.51 (± 0.01) g/cc cylinder 50.8 mm diam x 50.8 mm long.
b Tetryl as above, but cylinder 101.6 mm long.
c Velocity read from calibration curve, lowest curve in Fig. 9.
d Gap read for velocity (c) from upper curve of Fig. 10.
e Gap read for velocity (c) from middle curve of Fig. 9.
* Tetryl pellets used for all other experiments described in this report were from lot NP 1878-96. Pellets from each of these two lots, when used in the donor/Plexiglas configuration of the gap test, gave experimentally identical calibration curves.

DISTRIBUTION

	No. of Copies
CPIA (Distribution List)	132
Director, Special Projects Office Washington 25, D.C.	
Code 20	4
Code 271	1
Code 2710	1
Chief, Bureau of Naval Weapons Washington 25, D.C.	
DIS-3	4
RUME-32	1
RUME-33	1
RUME-21	1
RMMP-11	1
RRRE-6	1
Commanding Officer, Naval Propellant Plant Indian Head, Maryland	
Library Division	1
Process Development Division	1
W. C. Cagle	1
Commanding Officer Naval Explosive Ordnance Disposal Facility Indian Head, Maryland	
Library Division	1
U.S. Army Engineer Research and Development Labs. Fort Belvoir, Virginia	
STINFO Branch	1
U.S. Bureau of Mines 4800 Forbes Street, Pittsburgh 13, Pennsylvania	
Dr. C. M. Mason	1
Aerojet-General Corporation, Azusa, California	
R. F. Chaiken	1
Aerojet-General Corporation, Downey, California	
Dr. H. J. Fisher	3
Hercules Powder Company Allegany Ballistics Laboratory P.O. Box 210, Cumberland, Maryland	
Mr. Robert Richardson	1
Dr. Eyler	1
Dr. LeBlanc	1
Director, Office of the Secretary of Defense ARPA, Washington 25, D.C.	
Dr. John F. Kincaid	1
Atlantic Research Corporation 812 North Fairfax Street, Alexandria, Virginia	
Dr. Andrej Macek	1

DISTRIBUTION
(Cont)

	No. of Copies
University of Cal. Lawrence Radiation Lab. P.O. Box 1663, Los Alamos, New Mexico Dr. L. C. Smith	1
Space Technology Laboratory P.O. Box 95001, Los Angeles 45, California Mr. H. A. Taylor	1
Aerojet General Corporation Sacramento, California Dr. W. Kirchner	4
Lockheed Missiles and Space Company A Division of Lockheed Aircraft Corporation 1122 Jagels Road Sunnyvale, California Mr. J. Lightfoot	3
Bureau of Naval Weapons Representative (Special Projects Office) Lockheed Missiles and Space Company P.O. Box 504, Sunnyvale, California SPL-313	2
Bureau of Naval Weapons Representative (Special Projects Office) Aerojet-General Corporation Sacramento, California SPLA-30	2
Bureau of Naval Weapons Branch Representative Allegany Ballistics Laboratory SPH-30	2
Aeronutronics A Division of the Ford Motor Company Ford Road, Newport Beach, California Mr. W. Weller	2
Mr. M. Boyer	1
Rohm and Haas Company Redstone Arsenal, Huntsville, Alabama Dr. H. Shuey	3
Commander, U.S. Naval Ordnance Test Station China Lake, California Code 452	2
Code 5008	1
Armed Services Explosives Safety Board Building T-7, Gravelly Point Washington, D.C. Mr. R. C. Herman	1

DISTRIBUTION
(Cont.)

	No. of Copies
Stanford Research Institute Liquid Propellant Department Propulsion Services Division Menlo Park, California Dr. A. B. Amster	1
Defense Documentation Center Cameron Station Alexandria, Virginia	20
Office of Naval Research Washington 25, D.C. Code 429	2
University of Cal. Lawrence Radiation Laboratory P.O. Box 1663, Los Alamos, New Mexico R. Wasley	1

UNCLASSIFIED

Security Classification

DOCUMENT CONTROL DATA - R&D

(Security classification of title, body of abstract, and indexing annotation must be entered when the overall report is classified)

1 ORIGINATING ACTIVITY (Corporate author)
U.S. NAVAL ORDNANCE LABORATORY
WHITE OAK
SILVER SPRING, MARYLAND

2a REPORT SECURITY CLASSIFICATION
UNCLASSIFIED

2b GROUP
-

3 REPORT TITLE

THE EFFECTS OF CONFIGURATION AND CONFINEMENT ON BOOSTER CHARACTERISTICS

4 DESCRIPTIVE NOTES (Type of report and inclusive dates)
Final

5 AUTHOR(S) (Last name, first name, initial)
Jaffe, Irving (NMI)
Clairmont, A. Robert

6 REPORT DATE
1965 - 13 April 1965

7a TOTAL NO OF PAGES
31

7b NO OF REFS
7

8a CONTRACT OR GRANT NO

b PROJECT NO
NOrd-22 149/212 1/F009/06-11

c

d

9a ORIGINATOR'S REPORT NUMBER(S)
NOLTR 65-33

9b OTHER REPORT NO(S) (Any other numbers that may be assigned this report)
-

10 AVAILABILITY LIMITATION NOTICES
Qualified requesters may obtain copies of this report from DDC.

11 SUPPLEMENTARY NOTES
-

12 SPONSORING MILITARY ACTIVITY
Bureau of Naval Weapons
Washington, D.C.

13 ABSTRACT The purpose of this work was to examine the effect of certain changes in size, shape, and confinement on the effectiveness of tetryl boosters. Effectiveness was judged in two ways: by the booster's approximation to a plane-wave generator and by its initiating strength. Consequently the measurements made were of non-planarity (radius of curvature) of the detonation front emerging from the booster and of the shock velocity vs distance curves of the hydrodynamic disturbance it caused in Plexiglas.

The changes made in confinement and shape of two-inch diam boosters caused no significant change in either performance property. Changes in booster length, however, had a marked effect. Booster effectiveness increases with increasing length and is still increasing at ℓ/d of 4 contrary to literature statements that curvature of the detonation front is constant at $\ell/d \geq 3$ and that booster strength becomes constant at $\ell/d \geq 1.5$. The validity of using truncated cones in place of cylindrical boosters in large-scale field tests of detonability was confirmed. The variation of 50% gap thickness with booster length (and corresponding invariance of critical initiating pressure), for a given test material, was quantitatively measured.

DD Form 1473

UNCLASSIFIED

Security Classification

UNCLASSIFIED
Security Classification

14 KEY WORDS	LINK A		LINK B		LINK C	
	ROLE	WT	ROLE	WT	ROLE	WT
Tetryl						
Boosters						
Shock Sensitivity						
Conical Boosters						
Cylindrical Boosters						
Length/Diameter						
Gap Sensitivity						

INSTRUCTIONS

1. **ORIGINATING ACTIVITY** Enter the name and address of the contractor, subcontractor, grantee, Department of Defense activity or other organization (*corporate author*) issuing the report.

2a. **REPORT SECURITY CLASSIFICATION** Enter the overall security classification of the report. Indicate whether "Restricted Data" is included. Marking is to be in accordance with appropriate security regulations.

2b. **GROUP** Automatic downgrading is specified in DoD Directive 5200.10 and Armed Forces Industrial Manual. Enter the group number. Also, when applicable, show that optional markings have been used for Group 3 and Group 4 as authorized.

3. **REPORT TITLE** Enter the complete report title in all capital letters. Titles in all cases should be unclassified. If a meaningful title cannot be selected without classification, show title classification in all capitals in parenthesis immediately following the title.

4. **DESCRIPTIVE NOTES** If appropriate, enter the type of report, e.g., interim, progress, summary, annual, or final. Give the inclusive dates when a specific reporting period is covered.

5. **AUTHOR(S)** Enter the name(s) of author(s) as shown on or in the report. Enter last name, first name, middle initial. If military, show rank and branch of service. The name of the principal author is an absolute minimum requirement.

6. **REPORT DATE** Enter the date of the report as day, month, year, or month, year. If more than one date appears on the report, use date of publication.

7a. **TOTAL NUMBER OF PAGES** The total page count should follow normal pagination procedures, i.e., enter the number of pages containing information.

7b. **NUMBER OF REFERENCES** Enter the total number of references cited in the report.

8a. **CONTRACT OR GRANT NUMBER** If appropriate, enter the applicable number of the contract or grant under which the report was written.

8b, 8c, & 8d. **PROJECT NUMBER** Enter the appropriate military department identification, such as project number, subproject number, system numbers, task number, etc.

9a. **ORIGINATOR'S REPORT NUMBER(S)** Enter the official report number by which the document will be identified and controlled by the originating activity. This number must be unique to this report.

9b. **OTHER REPORT NUMBER(S)** If the report has been assigned any other report numbers (either by the originator or by the sponsor), also enter the number(s).

10. **AVAILABILITY/LIMITATION NOTICES** Enter any limitations on further dissemination of the report, other than those imposed by security classification, using standard statements such as:

(1) "Qualified requesters may obtain copies of this report from DDC."

(2) "Foreign announcement and dissemination of this report by DDC is not authorized."

(3) "U. S. Government agencies may obtain copies of this report directly from DDC. Other qualified DDC users shall request through

_____."

(4) "U. S. military agencies may obtain copies of this report directly from DDC. Other qualified users shall request through

_____."

(5) "All distribution of this report is controlled. Qualified DDC users shall request through

_____."

If the report has been furnished to the Office of Technical Services, Department of Commerce, for sale to the public, indicate this fact and enter the price, if known.

11. **SUPPLEMENTARY NOTES** Use for additional explanatory notes.

12. **SPONSORING MILITARY ACTIVITY** Enter the name of the departmental project office or laboratory sponsoring (paying for) the research and development. Include address.

13. **ABSTRACT** Enter an abstract giving a brief and factual summary of the document indicative of the report, even though it may also appear elsewhere in the body of the technical report. If additional space is required, a continuation sheet shall be attached.

It is highly desirable that the abstract of classified reports be unclassified. Each paragraph of the abstract shall end with an indication of the military security classification of the information in the paragraph, represented as (TS), (S), (C), or (U).

There is no limitation on the length of the abstract. However, the suggested length is from 150 to 225 words.

14. **KEY WORDS** Key words are technically meaningful terms or short phrases that characterize a report and may be used as index entries for cataloging the report. Key words must be selected so that no security classification is required. Identifiers, such as equipment model designation, trade name, military project code name, geographic location, may be used as key words but will be followed by an indication of technical context. The assignment of links, rules, and weights is optional.

Naval Ordnance Laboratory, White Oak, Md.
(NOL technical report 65-33)
THE EFFECTS OF CONFIGURATION AND CONFINEMENT ON BOOSTER CHARACTERISTICS, by I. Jaffe and A. R. Clairmont. 13 April 1965. 39p. illus., charts, tables. NuWeps task RMAT-32 149/212 1/F009/06-11.

UNCLASSIFIED

The purpose of this work was to examine the effect of certain changes in size, shape, and confinement on the effectiveness of tetryl boosters. Effectiveness was judged in two ways: by the booster's approximation to a plane-wave generator and by its initiating strength. Consequently the measurements made were of non-planarity (radius of curvature) of the detonation front emerging from the booster and of the shock velocity vs distance curves of the hydrodynamic disturbance it caused in plexiglas.

1. Boosters - Design
2. Boosters, Tetryl
I. Title
II. Jaffe, Irving
III. Clairmont, A. Robert, jt. author
IV. Project

Abstract card is unclassified.

Naval Ordnance Laboratory, White Oak, Md.
(NOL technical report 65-33)
THE EFFECTS OF CONFIGURATION AND CONFINEMENT ON BOOSTER CHARACTERISTICS, by I. Jaffe and A. R. Clairmont. 13 April 1965. 39p. illus., charts, tables. NuWeps task RMAT-32 149/212 1/F009/06-11.

UNCLASSIFIED

The purpose of this work was to examine the effect of certain changes in size, shape, and confinement on the effectiveness of tetryl boosters. Effectiveness was judged in two ways: by the booster's approximation to a plane-wave generator and by its initiating strength. Consequently the measurements made were of non-planarity (radius of curvature) of the detonation front emerging from the booster and of the shock velocity vs distance curves of the hydrodynamic disturbance it caused in plexiglas.

1. Boosters - Design
2. Boosters, Tetryl
I. Title
II. Jaffe, Irving
III. Clairmont, A. Robert, jt. author
IV. Project

Abstract card is unclassified.

Naval Ordnance Laboratory, White Oak, Md.
(NOL technical report 65-33)
THE EFFECTS OF CONFIGURATION AND CONFINEMENT ON BOOSTER CHARACTERISTICS, by I. Jaffe and A. R. Clairmont. 13 April 1965. 39p. illus., charts, tables. NuWeps task RMAT-32 149/212 1/F009/06-11.

UNCLASSIFIED

The purpose of this work was to examine the effect of certain changes in size, shape, and confinement on the effectiveness of tetryl boosters. Effectiveness was judged in two ways: by the booster's approximation to a plane-wave generator and by its initiating strength. Consequently the measurements made were of non-planarity (radius of curvature) of the detonation front emerging from the booster and of the shock velocity vs distance curves of the hydrodynamic disturbance it caused in plexiglas.

1. Boosters - Design
2. Boosters, Tetryl
I. Title
II. Jaffe, Irving
III. Clairmont, A. Robert, jt. author
IV. Project

Abstract card is unclassified.

Naval Ordnance Laboratory, White Oak, Md.
(NOL technical report 65-33)
THE EFFECTS OF CONFIGURATION AND CONFINEMENT ON BOOSTER CHARACTERISTICS, by I. Jaffe and A. R. Clairmont. 13 April 1965. 39p. illus., charts, tables. Bureau task RMAT-22 149/212 1/F009/06-11.

UNCLASSIFIED

The purpose of this work was to examine the effect of certain changes in size, shape, and confinement on the effectiveness of tetryl boosters. Effectiveness was judged in two ways: by the booster's approximation to a plane-wave generator and by its initiating strength. Consequently the measurements made were of non-planarity (radius of curvature) of the detonation front emerging from the booster and of the shock velocity vs distance curves of the hydrodynamic disturbance it caused in plexiglas.

1. Boosters - Design
2. Boosters, Tetryl
I. Title
II. Jaffe, Irving
III. Clairmont, A. Robert, jt. author
IV. Project

Abstract card is unclassified.

Naval Ordnance Laboratory, White Oak, Md.
(NOL technical report 65-33)
THE EFFECTS OF CONFIGURATION AND CONFINEMENT ON BOOSTER CHARACTERISTICS, by I. Jaffe and A. R. Clairmont. 13 April 1965. 39p. illus., charts, tables. Bureau task RMAT-22 149/212 1/F009/06-11.

UNCLASSIFIED

The purpose of this work was to examine the effect of certain changes in size, shape, and confinement on the effectiveness of tetryl boosters. Effectiveness was judged in two ways: by the booster's approximation to a plane-wave generator and by its initiating strength. Consequently the measurements made were of non-planarity (radius of curvature) of the detonation front emerging from the booster and of the shock velocity vs distance curves of the hydrodynamic disturbance it caused in plexiglas.

1. Boosters - Design
2. Boosters, Tetryl
I. Title
II. Jaffe, Irving
III. Clairmont, A. Robert, jt. author
IV. Project

Abstract card is unclassified.

Naval Ordnance Laboratory, White Oak, Md.
(NOL technical report 65-33)
THE EFFECTS OF CONFIGURATION AND CONFINEMENT ON BOOSTER CHARACTERISTICS, by I. Jaffe and A. R. Clairmont. 13 April 1965. 39p. illus., charts, tables. Bureau task RMAT-22 149/212 1/F009/06-11.

UNCLASSIFIED

The purpose of this work was to examine the effect of certain changes in size, shape, and confinement on the effectiveness of tetryl boosters. Effectiveness was judged in two ways: by the booster's approximation to a plane-wave generator and by its initiating strength. Consequently the measurements made were of non-planarity (radius of curvature) of the detonation front emerging from the booster and of the shock velocity vs distance curves of the hydrodynamic disturbance it caused in plexiglas.

1. Boosters - Design
2. Boosters, Tetryl
I. Title
II. Jaffe, Irving
III. Clairmont, A. Robert, jt. author
IV. Project

Abstract card is unclassified.

DISCLAIMER NOTICE

THIS DOCUMENT IS BEST QUALITY PRACTICABLE. THE COPY FURNISHED TO DTIC CONTAINED A SIGNIFICANT NUMBER OF PAGES WHICH DO NOT REPRODUCE LEGIBLY.